Full Articles

Theoretical study of oxidation of molecular nitrogen with vanadium peroxo complexes

A. F. Shestakov and N. S. Emelyanova

Institute of Problems of Chemical Physics, Russian Academy of Sciences, 142432 Chernogolovka, Moscow Region, Russian Federation. Fax: +7 (096) 515 3588. E-mail: as@icp.ac.ru

The structure and reactivity toward molecular nitrogen of vanadium diperoxo complexes, as well as the influence of the protonation and coordination of trifluoroacetate on the reactivity, were studied using the density functional method. The most stable form of the starting complex is the ozonide $[V(O_3)O_2]^-$. The triplet state of the complex is formed with small energy expenses for electron transfer from the peroxo ligand to the vanadium atom to form V^{IV}. The transfer of the O atom to the N_2 molecule to form N_2O is possible for several transition states. The nature of possible complexes and transition states retains upon protonation but the number of different structures increases depending on the ligand and the site of proton addition. Upon protonation the reactivity increases and the lowest activation barrier decreases from 27 to 20 kcal mol^{-1}. The coordination of trifluoracetate anion also decreases the activation barrier for the intermolecular transfer of oxygen to the nitrogen molecule.

Key words: vanadium peroxo complexes, vanadium ozonides, dinitrogen oxidative activation, quantum-chemical calculations, density functional theory.

Vanadium peroxo complexes are efficient oxidizing agents for various organic compounds under mild conditions.[1] Active sites of enzymes, *viz.*, haloperoxidases that perform the oxidative halogenation of substrates, contain these complexes.[2—4] We have previously[5] examined the possibility of oxidative dinitrogen activation to form N_2O and concluded, on the basis of calculations of the model systems, a considerable decrease in the activation barrier of the O atom transfer from the peroxo ligand to the dinitrogen molecule in the coordination sphere of metal complexes. Therefore, vanadium peroxo complexes are of high interest as potential oxidizing agents for dinitrogen.

Complexes formed in the $V^V—H_2O_2—CF_3COOH$ system attract special attention due to their ability to perform molecular oxidation.[6,7] In the absence of substrates, H_2O_2 is decomposed not only according to the most thermodynamically favorable reaction

$$H_2O_2 \longrightarrow H_2O + 1/2\ O_2,\ \Delta H^\circ_{f,\,298} = -23.5\ \text{kcal mol}^{-1},$$

but also with the formation of ozone

$$H_2O_2 \longrightarrow H_2O + 1/3\ O_3,\ \Delta H^\circ_{f,\,298} = -12.2\ \text{kcal mol}^{-1},$$

and singlet molecular oxygen[8,9]

$$H_2O_{2(l)} \longrightarrow H_2O_{(l)} + 1/2\ O_2\ (^1\Delta_g),$$

$$\Delta H^\circ_{f,\,298} = -0.9\ \text{kcal mol}^{-1}.$$

Published in Russian in *Izvestiya Akademii Nauk. Seriya Khimicheskaya,* No. 7, pp. 1375—1391, July, 2003.

1066-5285/03/5207-1455 $25.00

In two latter reactions, hydrogen peroxide does not completely use its oxidative potential. Therefore, the transfer of the O atom to the nitrogen molecule can be expected under these conditions

$$H_2O_{2(l)} + N_2 \longrightarrow H_2O_{(l)} + N_2O,$$

$$\Delta H^\circ_{f,\,298} = -3.9 \text{ kcal mol}^{-1},$$

which is also characterized by a small energy gain.

The first experimental studies[10] have confirmed this expectations. In this work, we theoretically studied possible routes for the formation of N_2O from N_2 and the vanadium peroxo complexes.

Procedure of calculation

Calculations were performed by the B3LYP hybrid DFT methods using the GAUSSIAN 98 program.[11] The geometry of the stationary states was optimized in the LANL2DZ basis set, and the character of the structure obtained (minimum or transition state) was confirmed by the calculation of frequencies in the harmonic approximation. The resulting geometry was used to calculate the energy of the system in the extended LANL2DZ basis set augmented by the diffusion and polarization functions for all atoms, which were the same as those in the 6-311++(d,p) basis set.

Choice of the model

Vanadium(v) interacts with H_2O_2 to form a number of mononuclear[12—17] and polynuclear[18—22] complexes, which differ by the charge and number of the peroxo groups per vanadium atom (from 1 to 4). When direct experimental data are absent, it is rather difficult to choose an active species for studying its reactivity toward dinitrogen. Since the purpose of this work was to reveal the factors decreasing the activation energy of the O atom transfer from the coordination sphere of V^V to the N_2 molecule, the choice of a specific vanadium complex was not so important. In this work, we considered in detail the structures of different isomers of the $V(O_2)_2O^-$ diperoxo complex and its protonated form and their possible reactions with N_2. The effects of nonspecific solvation with CF_3COOH and specific solvation through the complex formation of one CF_3COO^- anion at the vanadium atom were also studied.

A few works were devoted to the quantum-chemical studies of the vanadium peroxo complexes.[23—26] The authors of these works studied mainly the thermodynamic and structural aspects of mutual transformations of these complexes with a change in the number of the peroxo groups or solvent molecules in the coordination sphere and did not consider the reactivity of the complexes. In order to verify the accuracy of the approach used, we considered the X-ray diffraction characterized $[VO(O_2)_2(NH_3)]^-$ peroxo complex.[27] A comparison of the calculated bond lengths and angles with the experimental values (Table 1) showed that the difference in the valent distances is very small: on the average, 0.026 Å. The average difference in the bond angles is greater: 5°, which is likely related to the easy angular deformation of the complex in the field of the $[VO(O_2)_2(NH_3)]^-[NH_4]^+$ ionic crystal.

Table 1. Comparison of the calculated[a] and experimental[b] bond lengths (d) and angles (ω) in the $[V{=}O_a(O_b{-}O_c)_2NH_3]^-$ complex

Bond	d/Å		Angle	ω/deg	
	Experiment	Calculation		Experiment	Calculation
$V{-}O_a$	1.599	1.620	$O_a{-}V{-}O_b$	105.4	110.0
$V{-}O_b$	1.871	1.901	$O_a{-}V{-}O_c$	106.3	112.2
$V{-}O_c$	1.872	1.874	$O_a{-}V{-}N$	97.5	91.6
$V{-}N$	2.098	2.155	$O_b{-}V{-}O_c$	46.0	47.5
$O_b{-}O_c$	1.463	1.521	$O_b{-}V{-}N$	128.5	127.1
			$O_b{-}V{-}O_b$	88.9	90.7
			$O_c{-}V{-}N$	83.6	79.7
			$O_c{-}V{-}O_c$	146.3	131.2

[a] This work.
[b] The data in Ref. 27.

Results of calculation

System $VO_5^- + N_2$. The results of calculation of the stationary points in the $VO_5^- + N_2$ system are presented in Table 2. The potential energy diagram for the $VO_5^- + N_2$ system is shown in Fig. 1. Several structures were optimized in the extended basis set (energies are presented in Table 3). As should be expected, the total energies change insignificantly, indicating the minimum changes in the geometry of this optimization. The relative energies of the structures change by at most 2 kcal mol^{-1}, with the only exception for the transition state **TS$_3$**, which is destabilized by 5 kcal mol^{-1}.

Complex **1** with ozone is characterized by the lowest energy in the system (Fig. 2), lying in the energy scale by 1.1 kcal mol^{-1} lower than diperoxo complex **2**. It is of interest that the triplet form of diperoxo complex **2T** is formed with the expense of only 13.5 kcal mol^{-1}. The spin and electron density distributions (see Fig. 2) show that the formation of this complex is accompanied by intramolecular redox transition. The complex can be considered as $V^{IV}(O_2^-)$, although the total charges on the O_2^- and O_2^{2-} ligands do not differ strongly, despite noticeable elongation of the V—O bonds from 1.83—1.89 Å to 2.07 Å and shortening of the O—O bond in the O_2^- ligand to 1.403 Å, which is close to its value in O_2^- (1.419 Å) calculated in the same B3LYP/LANL2DZ approximation. The complexes with the monodentate coordination of the peroxo group, *viz.*, triplet **3T** and singlet **3**, are

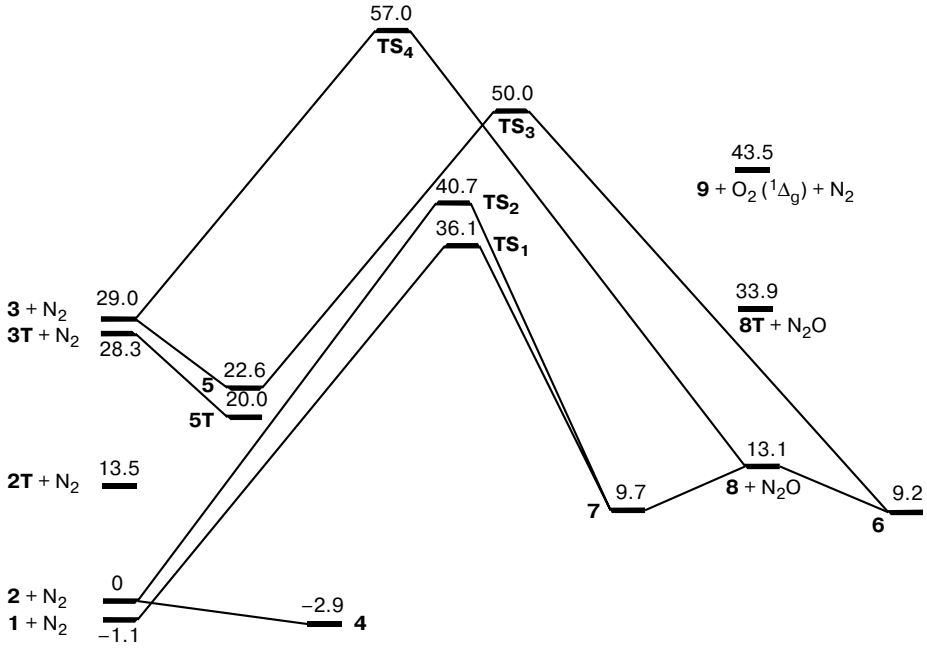

Fig. 1. Energy diagram for the $VO_5^- + N_2$ system.

Table 2. Total energies (E, E^*) and zero-point vibration energies ZPE of the vanadium complexes, transition states in the $VO_5^- + N_2$ system calculated by the B3LYP methods in the LANL2DZ basis set (E) and in the extended basis (E^*), and relative energies Δ

Structure	$-E$	ZPE	$-E^*$	Δ /kcal mol^{-1}
	hartree			
1	447.50392	0.01447	447.59264	−1.1
2	447.49353	0.01426	447.59052	0
2T	447.47427	0.01319	447.56788	13.5
3	447.44929	0.01345	447.54353	29.0
3T	447.45582	0.01292	447.54402	28.3
4	556.98724	0.02173	557.13813	−2.9
5	556.95216	0.02135	557.09709	22.6
5T	556.95691	0.02010	557.09998	20.0
TS_1	556.93787	0.02011	557.07442	36.1
TS_2	556.93098	0.02026	557.06724	40.7
TS_3	556.91391	0.02178	557.05395	50.0
TS_4	556.90482	0.01943	557.04033	57.0
6	556.9688	0.02307	557.12021	9.2
7	556.96479	0.02278	557.11913	9.7
8	372.34172	0.01148	372.41823	13.1
8T	372.30961	0.01056	372.38424	33.9
9	297.16228	0.00835	297.22060	43.5 [a]
10T	297.03851	0.00753	297.09709	120.6 [a]
11T	296.95601	0.00664	297.01572	171.4 [a]

[a] The relative energies were calculated under the assumption of singlet dioxygen formation in the system $VO_5^- \rightarrow VO_3^- + O_2$ ($^1\Delta_g$).

Table 3. Total energies E^*_{opt} and zero-point vibration energies ZPE* of the vanadium complexes, transition states in the $VO_5^- + N_2$ system calculated by the optimization of the geometry using the B3LYP method in the extended basis set (E^*), and their total energies calculated taking into account the solvation effects of CF_3COOH E^*_{solv}

Structure	$-E^*_{opt}$	ZPE*	$-E^*_{solv}$
	hartree		
2	447.59551	0.01479	447.59588
3	447.54799	0.01391	447.54907
4	557.14477	0.02267	557.14909
5	557.1036	0.02212	557.10787
TS_3	557.06027	0.02273	557.06099
TS_4	557.04469	0.02001	557.0462
6	557.12724	0.02426	557.13956
8	372.42097	0.01171	372.42101

higher in the energy scale. Their energies differ insignificantly; as in structure **2**, electron transfer from O_2^{2-} to V^V elongates the V—O bond and shortens the O—O bond.

The $VO(O_2)^{2-}$ complex has a coordination vacancy, although the bonding energy of the N_2 molecule is very small: only 2.9 kcal mol^{-1} at the rather short distance d(V—N) = 2.274 Å (Fig. 3). The $V(O_2)(O_3)^-$ complex with N_2 was not localized. It is most likely that a weak van der Waals complex is formed in this case. As known,[28] the formation of strong complexes with dinitrogen is favored by the π-donor properties of the metal center, which are

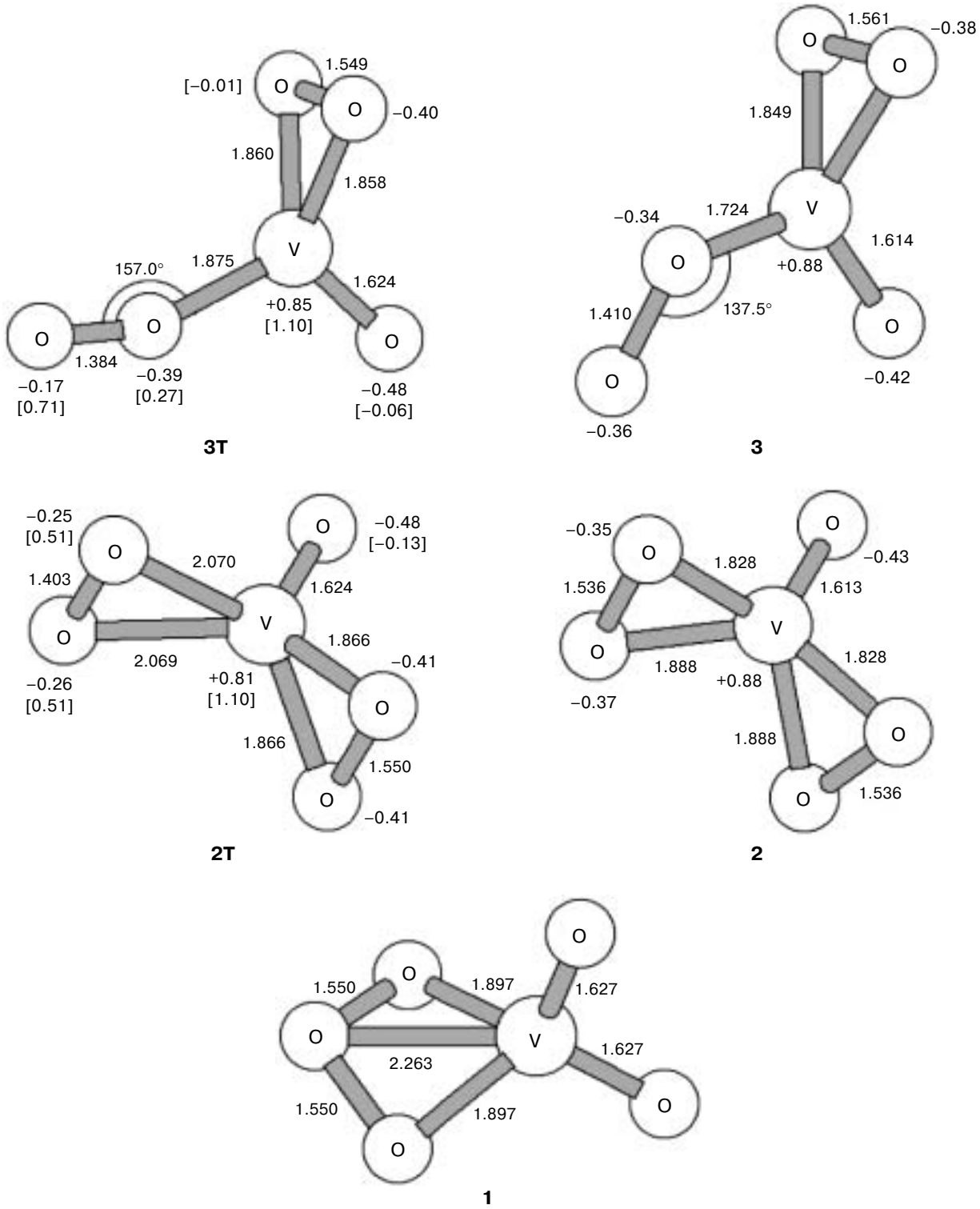

Fig. 2. Structures of the VO_5^- complexes. The figures without parentheses (with signs + and −) are the atom charges, and the figures in parentheses are the spin density values.

not characteristic of the vanadium atom in its highest oxidation state with the d^0 electron configuration. That is why the d^1-coordination center of the V^{IV} atom in structure **3T** is capable of forming a substantially more stable complex **5T** with the N_2 molecule (d(V—N) = 2.138 Å) characterized by a dissociation energy of 8.3 kcal mol^{-1}.

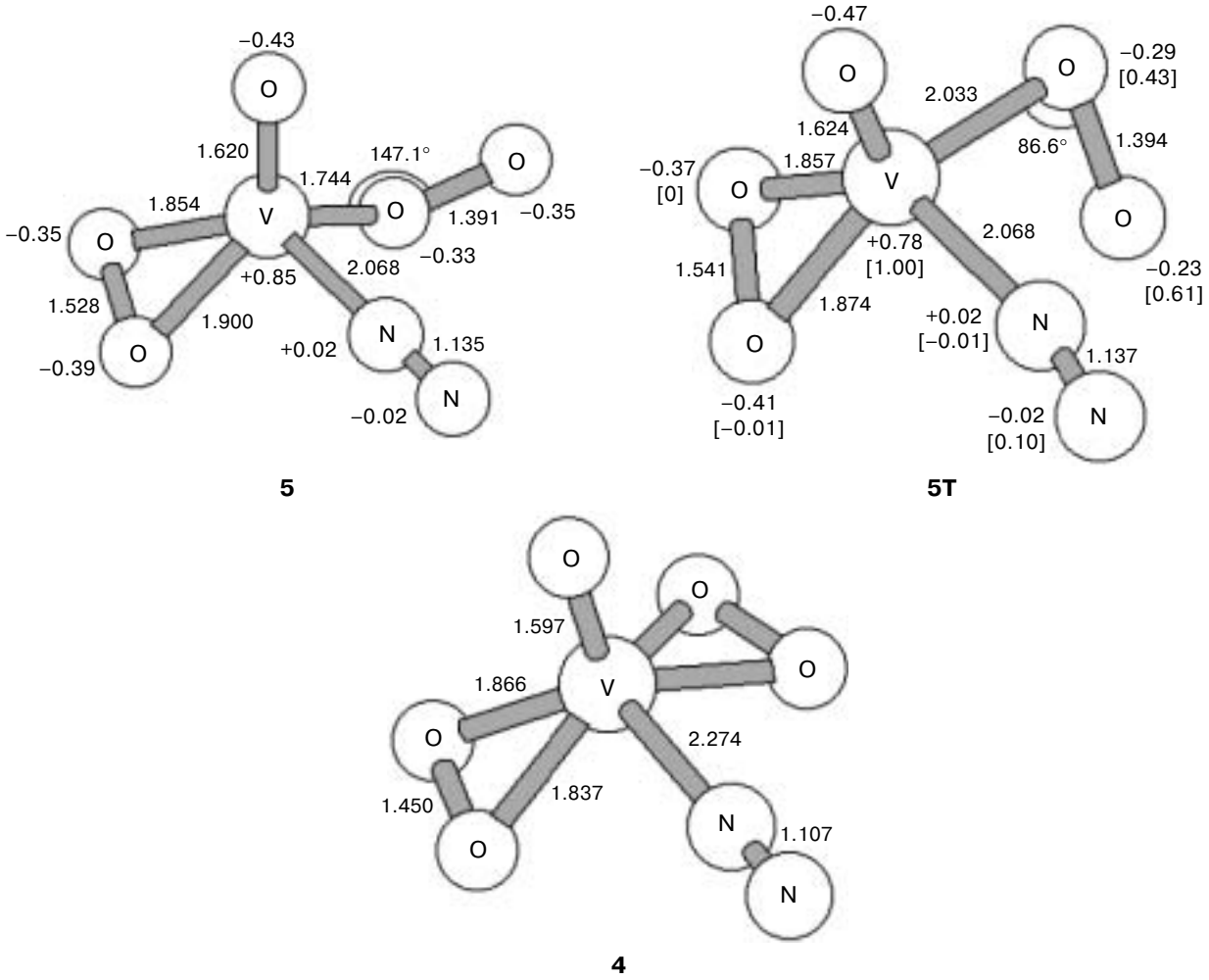

Fig. 3. Structures of the $VO_5(N_2)^-$ complexes. The figures without parentheses (with signs + and −) are the atom charges, and the figures in parentheses are the spin density values.

A close value of 6.4 kcal mol^{-1} was obtained for the singlet complex **5** (d(V—N) = 2.068 Å). Based on these data, we can consider both structures (**3** and **3T**) as the V^{IV} complexes with O_2^- characterized by a sufficiently small singlet-triplet splitting at different orientations of the spins localized on the V and terminal O atoms. As a whole, unstable complexes **4**, **5**, and **5T** are characterized by insignificant changes in the geometry upon dinitrogen coordination: the bond lengths change by at most 0.04 Å.

A study of the reactivity of the VO_5^- complex toward the N_2 molecule revealed several transition states (Fig. 4). Among them, the lowest energies are inherent in the transition states $\mathbf{TS_1}$ and $\mathbf{TS_2}$ in which the dinitrogen molecule is attacked by the O atom of the peroxo or trioxo ligand bound to the metal atom to form complex **7**, *viz.*, the N_2O molecule coordinated through the O atom (Fig. 5). However, the energy barriers are rather high: 37.2 and 40.7 kcal mol^{-1}, respectively.

The monodentate-coordinated peroxo group is highly reactive. The transition states formed by the intramolecular ($\mathbf{TS_3}$) and intermolecular ($\mathbf{TS_4}$) transfers of the O atom are characterized by much lower activation barriers of 27.4 and 28.0 kcal mol^{-1}, respectively. The nonlinear structure of the O—O—N—N group in complex $\mathbf{TS_4}$ resembles the transition state of O atom transfer from O_2^- to the N_2 molecule when the angles O—O—N 146° and O—N—N 139° are formed. The reaction products are the **6**—N_2O complex coordinated through the terminal N atom[6] or the free N_2O molecule and monoperoxo complex **8**. The energy of its bonding with N_2O is low: ~4 kcal mol^{-1} for different types of coordination. Due to a considerable loss in translation entropy of the N_2O molecule, the entropy of the system decreases by ~30 e.u. Therefore, the formation constants of these complexes are low and in fact they are not formed in noticeable amounts. The same is valid for the complexes with molecular nitrogen **4**, **5**, and **5T**. In particular, when complex **5** is formed from complex **3** and N_2, the standard entropy of the system decreases by 33 e.u., and the total change in the standard free energy calculated taking into

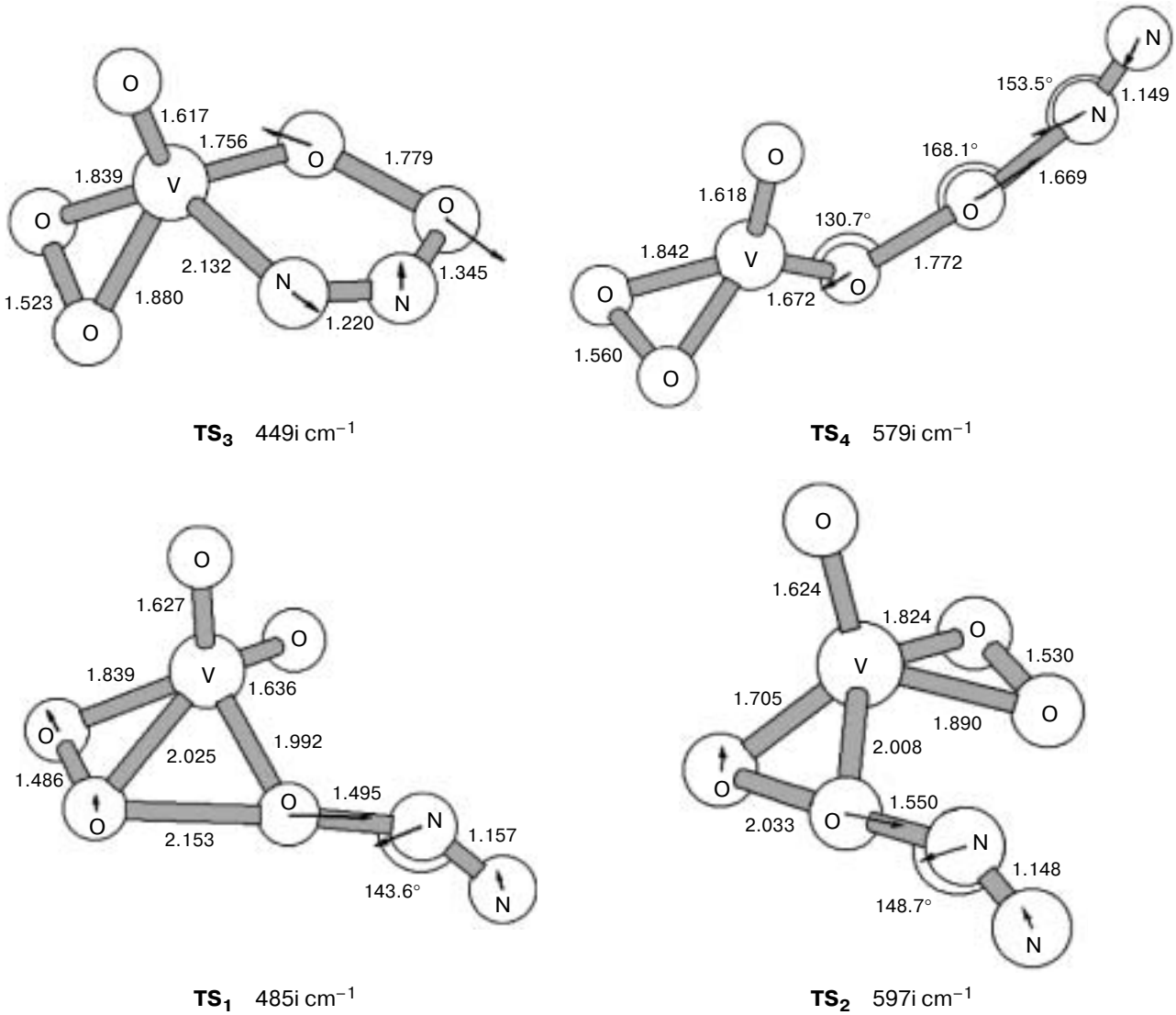

Fig. 4. Structures of the transition states in the $VO_5^- + N_2$ system. The arrows designate the displacements of the atoms for the vibration with the imaginary frequency.

account the temperature corrections to the thermal energy is +3 kcal mol^{-1}. Therefore, the formation of precursor complex **5** can be ignored in calculation of the energy barrier. This decreases to 21.0 kcal mol^{-1} the activation energy for the cyclic transition state **TS$_3$**. Taking into account that the activation energy may somewhat decrease upon the coordination of a solvent, the value obtained for the energy barrier can explain the high reactivity of the vanadium peroxo complexes toward N_2.

Transitions states **TS$_1$** and **TS$_2$** are closest in energy to structure **3**. It can be expected that the barrier for the transformation of the open form of complex **3** into closed form **2** is low, because the corresponding reaction coordinate mainly coincides with the rotation of the peroxo ligand. Moving from this barrier under continuing interaction with the dinitrogen molecule, one could, in principle, reach **TS$_2$** through the second-order saddle point and then can reach complex **6**. However, we did not attempt to locate this saddle point.

The open form of the complex possesses an excess energy. However, since ozone and singlet dioxygen are formed in the V^V—H_2O_2—CF_3COOH system, it can be concluded that energy-rich vanadium complexes (20—25 kcal mol^{-1}) are really formed in this system. The thermodynamically favorable decomposition of H_2O_2 is the source of the excess energy. According to the data of calculation, the formation of singlet dioxygen from the open form of diperoxo complex **3** requires low energy expenses: 14.5 kcal mol^{-1}, if it is accompanied by simultaneous transformation of the peroxo group into two oxo groups (complex **9**). The standard free energy increases only by 5.2 kcal mol^{-1}. The energy of the triplet $VO(O_2)^-$

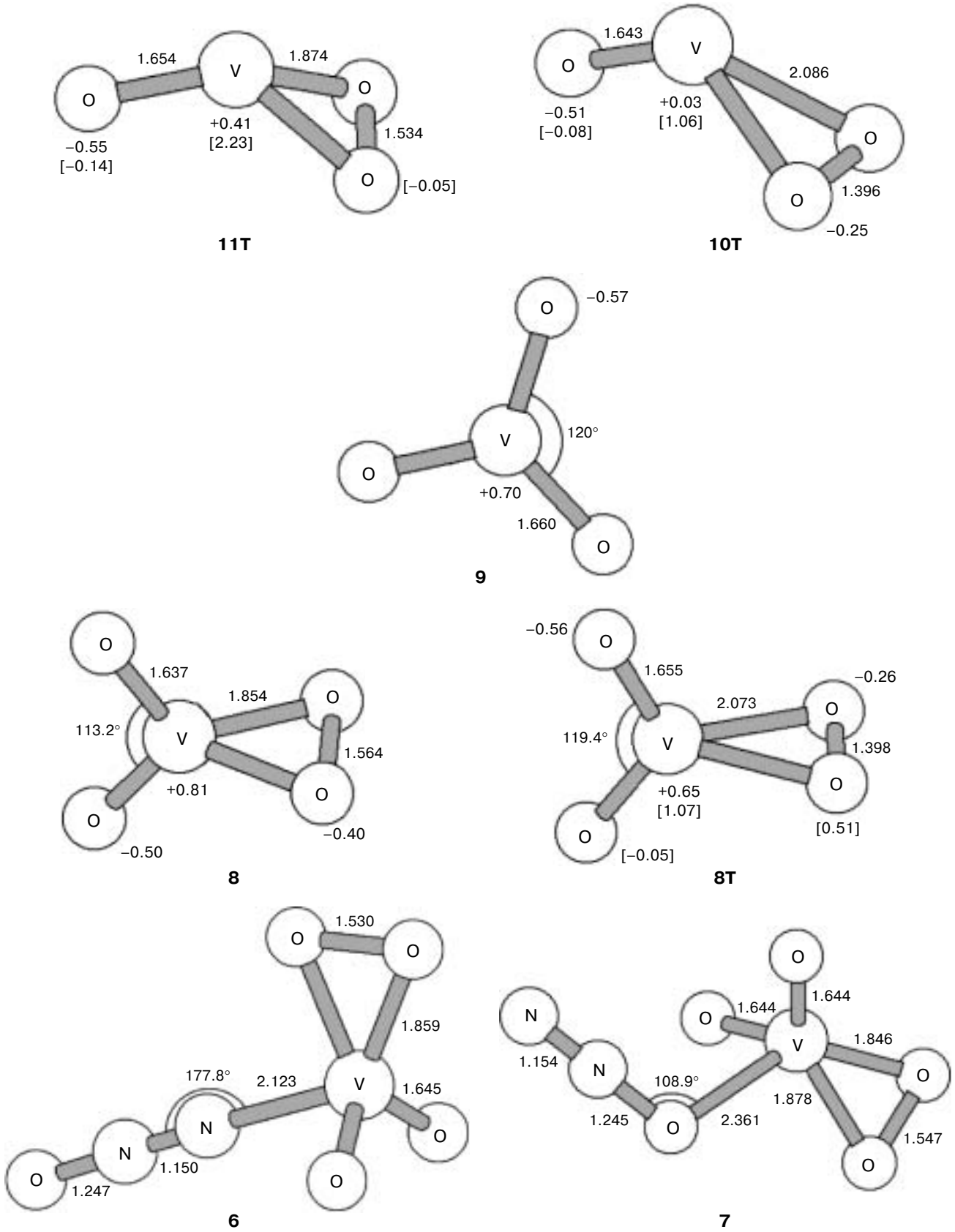

Fig. 5. Structures of the VO_3^-, VO_4^-, and $VO_4(N_2O)^-$ complexes.

peroxo complex **10T** is much higher than the energy of complex **9**. In this complex, as can be seen from the spin density distribution (see Fig. 5), the oxidation state of the vanadium atom bearing one unpaired electron is +4. The isomeric structure **11T** is still higher in energy, and the spin density distribution corresponds to the oxidation state of vanadium +3. However, this structure is characterized by one imaginary frequency. The alternative dissociation of the triplet complex **3T** to form the singlet dioxygen and triplet peroxo complex **10T** requires high energy expenses (~90 kcal mol^{-1}), which could be compensated in solution, to a great extent, by the formation of bonds with the solvent molecules in coordinately unsaturated complex **10T**.

In the isolated VO_5^- + N_2 system, the formation of N_2O is thermodynamically favorable when starting from the energy-rich peroxo complexes **2T**, **3**, and **3T**. Taking into account nonspecific effects of CF_3COOH solvation by the Onsager model does not change the situation. The solvation energies calculated using the effective dielectric constant of CF_3COOH [29] are presented in Table 3. It is seen that the energy shift is almost the same for all species, except for the product of the reaction of complex **8**.

System VO_5^- + CF_3COO^- + N_2. Solvent molecules are capable of specific interacting with the considered vanadium peroxo complexes, which contain coordination vacancies. As the first step, we performed calculations for complexes **2**, **3**, **8**, and **10** and transition state **TS_4** under the assumption of additional coordination of the CF_3COO^- ligand. The results are presented in Table 4 and in Figs. 6 and 7 and show that the open form of vanadium diperoxo complex **13** is characterized by a higher energy of interaction with trifluoroacetate anion, the latter decreasing the energy relatively to close form **12** by 10.4 kcal mol^{-1}. This is also reflected as the shortening of the V—O(CF_3COO) distance in complex **13** (2.04 Å) compared to that in complex **12** (2.13 Å). Despite the coordination vacancy in complex **13**, no bidentate CF_3COO^- coordination is observed for thic complex and final complex **14**. This conclusion agrees with the structural data,[30] according to which the monodentate coordination of the carboxylate groups is retained in the five-coordinate vanadium peroxo complexes. The transition state of the oxygen atom transfer to the N_2 molecule, as can be seen from the data in Fig. 7, acquires the later character, which results, most likely, in a small decrease in the activation barrier (only by 2.9 kcal mol^{-1}) for the coordination of the CF_3COO^- ligand.

Table 4. Total energies E and zero-point vibration energies ZPE of the vanadium complexes, transition states in the $VO_5CF_3COO^{2-}$ + N_2 system calculated using the B3LYP method in the LANL2DZ basis set and in the extended basis set (E*), and relative energies Δ

Structure	$-E$	ZPE	$-E$*	Δ /kcal mol^{-1}
	hartree			
12	973.67918	0.03997	973.92818	0.0
13	973.65138	0.03927	973.89787	18.6
TS_5	1083.11340	0.04546	1083.39930	43.9
14	898.52929	0.03707	898.75770	11.9
15	823.37039	0.03459	823.58070	30.0 [a]

[a] The relative energies were calculated under the assumption of singlet dioxygen formation in the system $VO_5CF_3COO^{2-} \rightarrow VO_3CF_3COO^{2-} + O_2$ ($^1\Delta_g$).

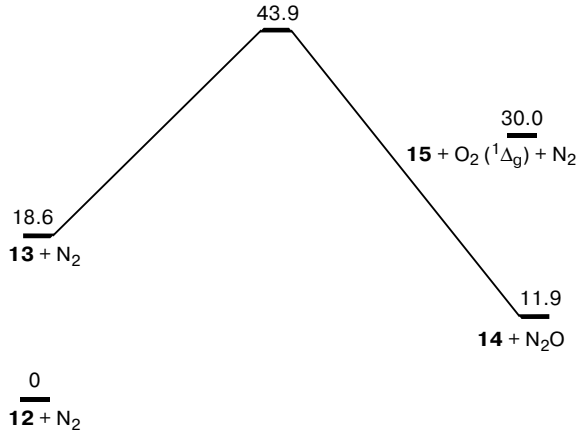

Fig. 6. Energy diagram for the $VO_5(CF_3COO)^{2-}$ + N_2 system.

System VO_5H + N_2. During the coordination of the H_2O_2 molecules with V^V, they dissociate with the escape of a proton into the solvent bulk,[25] although the inverse process, formation of the protonated forms of the peroxo complexes, is known for acidic media.[25] The formation of the intermolecular hydrogen bond between the peroxo ligand and carboxylic acid is also known.[31] The vanadium hydroperoxo complexes are characterized[25] by the enhanced reactivity in the decomposition of the complexes and uracil oxidation. The system under study contains a sufficiently strong acid. Therefore, we studied the effect of protonation on the structure and reactivity of the vanadium diperoxo complexes. According to the results of calculation, VO_5^- is only slightly, by 8.8 kcal mol^{-1}, inferior to the CF_3COO^- anion in the proton affinity.

The characteristic feature of the neutral VO_5H system is a great number of structures with close energies (Fig. 8). Complex **16** formed by the protonation of the oxo ligand in ozone-containing complex **1** is characterized by the lowest energy. The alternative protonation of the trioxo ligand affords complex **21**, whose energy is 22 kcal mol^{-1} higher. On the contrary, protonation at the peroxo group to form complex **17** is most favorable for diperoxo complex **2**. This specific feature has previously been mentioned[25] for the proton addition to vanadium aquamonoperoxo complexes. It is interesting that different types of protonation of complex **2**, resulting in the *cis*- and *trans*-arrangements of the V—O and O—H bonds (struc-

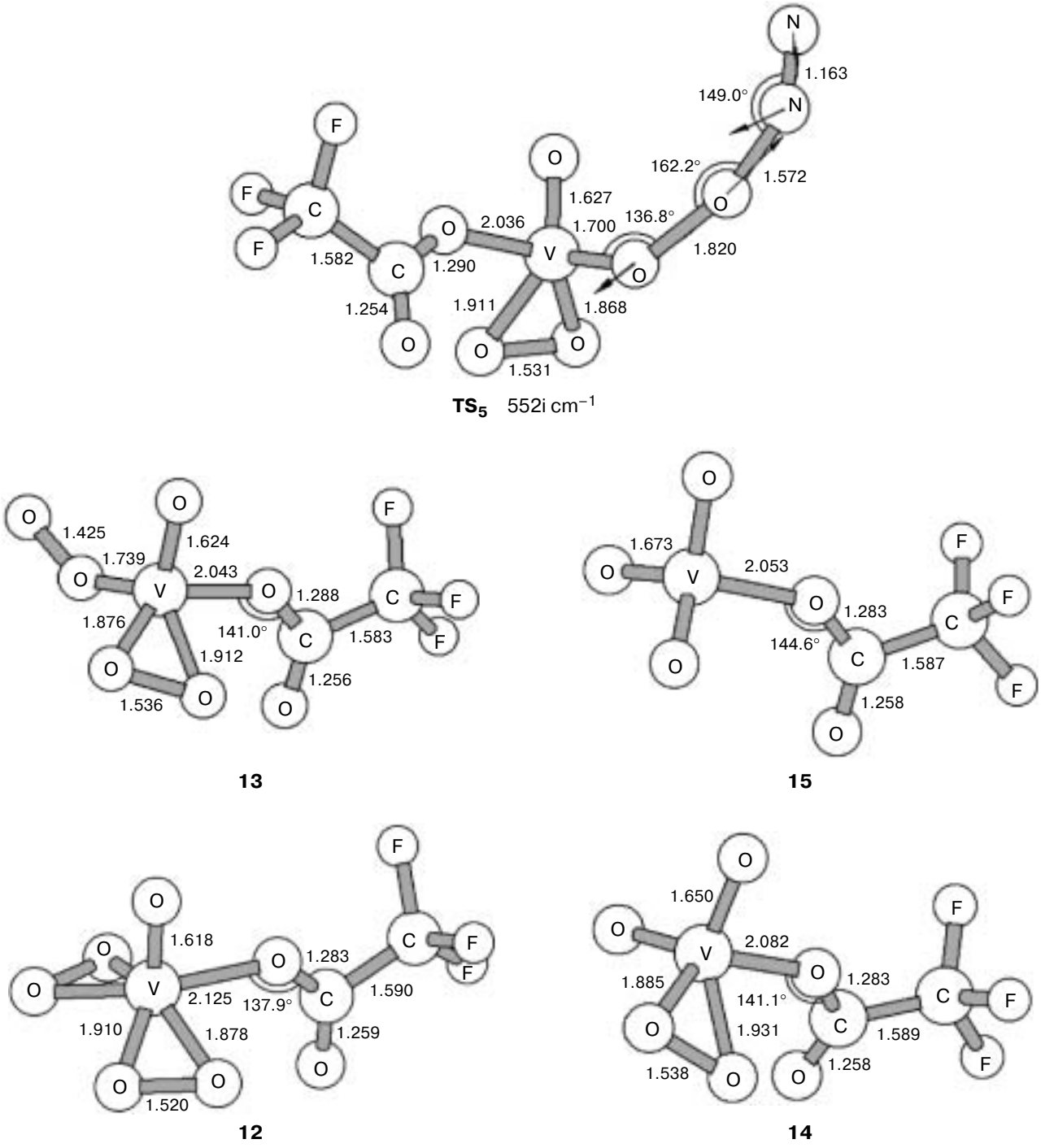

Fig. 7. Structures of the initial, final, and transition states in the $VO_5(CF_3COO)^{2-} + N_2$ system. The arrows designate the displacements of the atoms for the vibration with the imaginary frequency.

tures **17** and **20**, respectively), provide a noticeable difference in the energy of these complexes (8.9 kcal mol^{-1}), despite small differences in the bond lengths (Fig. 9). The greatest difference in the energy (25.3 kcal mol^{-1}) is observed for the protonation of the open form of VO_5^- to form the monodentate hydroperoxo ligand in structure **19** and the hydroxo ligand in structure **22**. A comparison of structures **17** and **19** shows that the closed form of the hydroperoxo complex is the most favorable, although the difference in these energies is rather small (6.8 kcal mol^{-1}). The neutral VO_5H complexes exhibit the higher affinity to the N_2 molecule in comparison with their negatively charged analogs. The greatest increase in the complex formation energy is observed for the base form of the

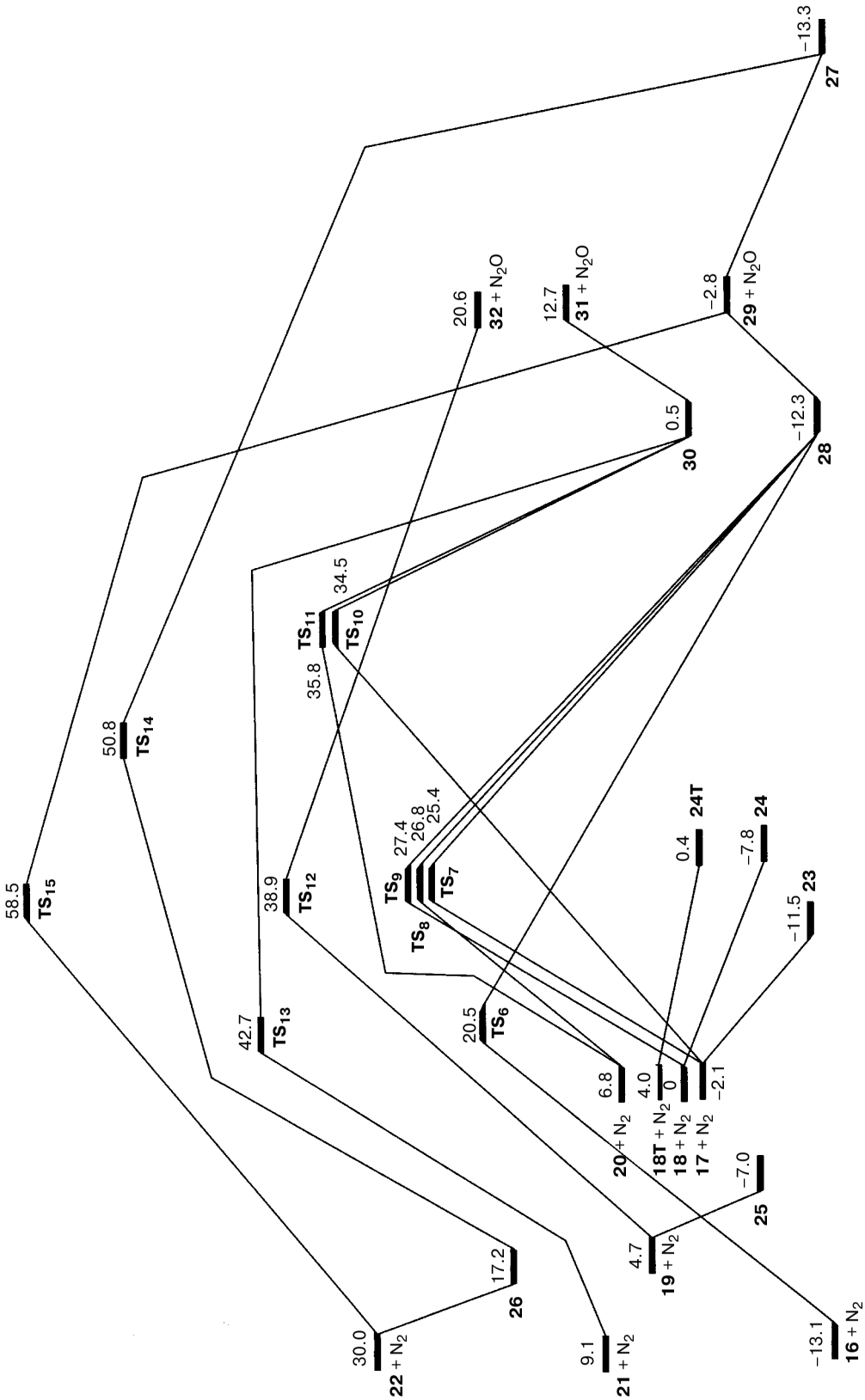

Fig. 8. Energy diagram for the $VO_3H + N_2$ system.

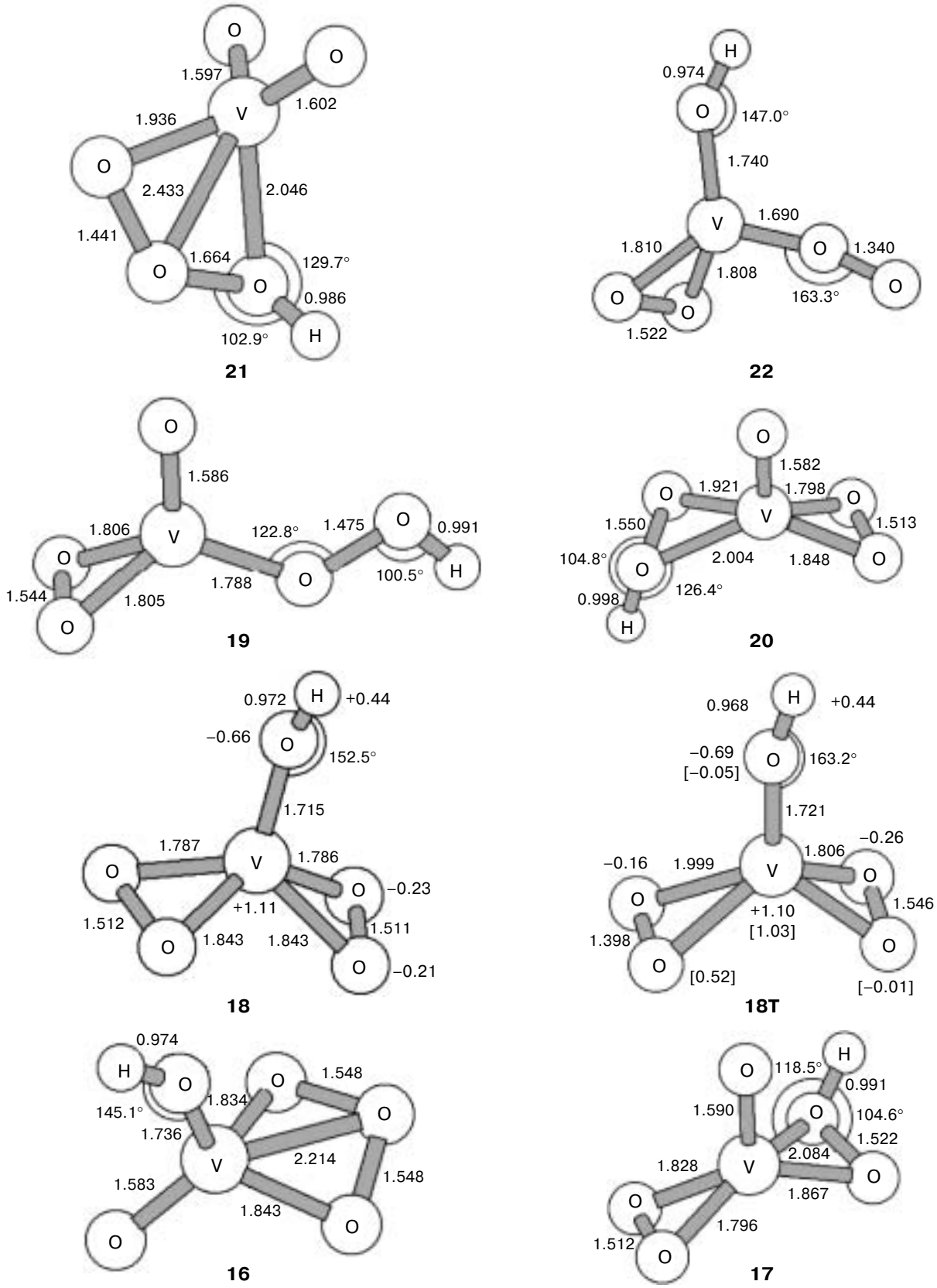

Fig. 9. Structures of the VO_5H complexes. The figures without parentheses (with signs + and −) are the atom charges, and the figures in parentheses are the spin density values.

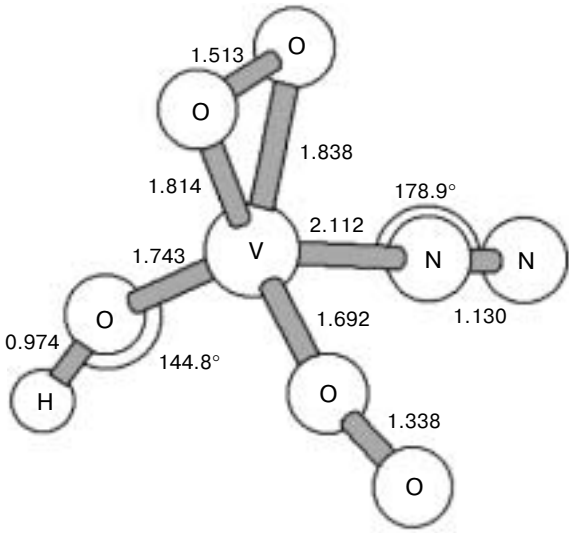

26

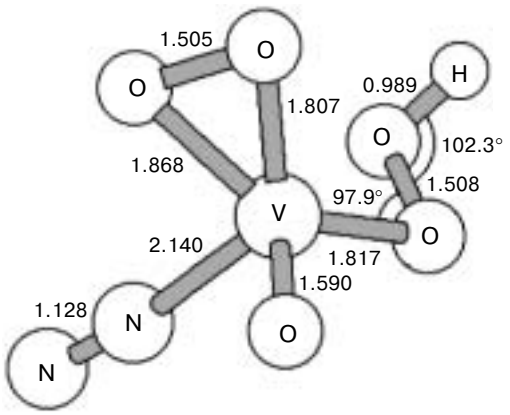

25

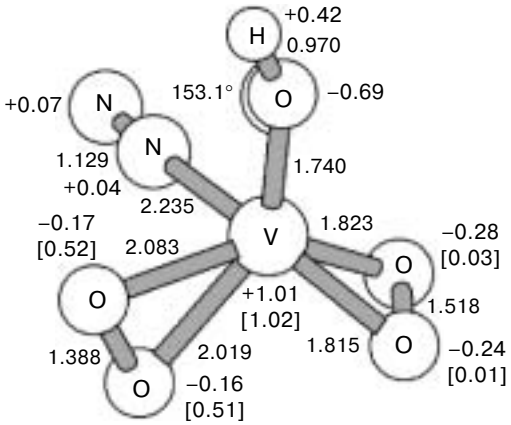

24T

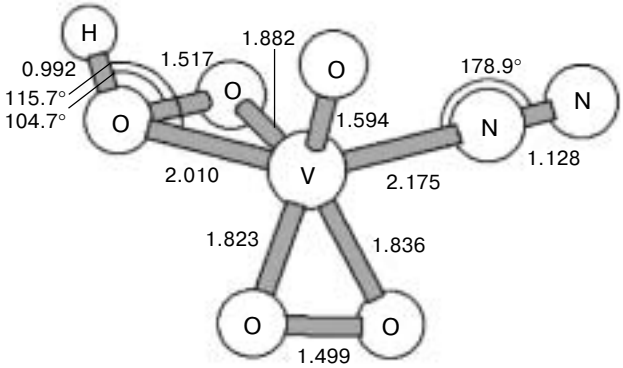

23

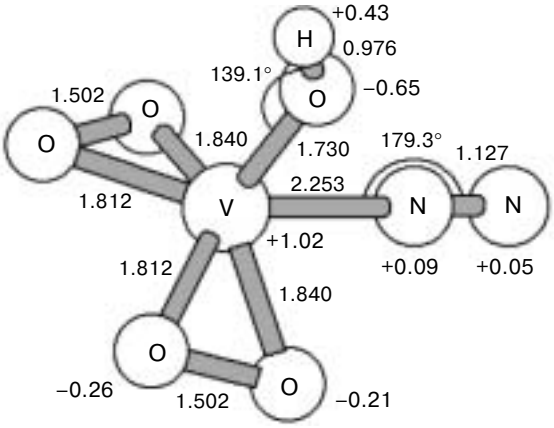

24

Fig. 10. Structures of the $VO_5H(N_2)$ complexes. The figures without parentheses (with signs + and –) are the atom charges, and the figures in parentheses are the spin density values.

diperoxo complex: from 2.9 to 9.4 kcal mol^{-1} in structure **23** and to 7.8 kcal mol^{-1} in structure **24**. The reason for this phenomenon is not quite clear because the donor ability of the vanadium complexes decreases, generally speaking, upon protonation. Perhaps, the π-donor ability of the metal is enhanced upon the formation of the O—H bond due to a nonlinear character of the V—O—H group. As can be seen from the comparison of the data in Figs. 10 and 3, this conclusion is reasonable because protonation somewhat shortens the V—N and and as a rule elongates the N—N bonds, despite an increase in the charge on the N_2 ligand.

Triplet complex **18T** and its negatively charged analog **2T** contain one peroxo group with the shortened O—O distance (1.40 Å), the elongated V—O (2.00 Å) distance, and one unpaired electron on the V atom.

When dinitrogen is oxidized to N_2O with the neutral VO_5H complexes, the types of transition states are the same (Fig. 11) as those for the anionic VO_5^- complexes. Depending on the sites of proton addition to the oxo, peroxo, or trioxo ligands, each of them can exist as several structures. The transition state **TS$_6$**, which appears upon the transfer of the oxygen atom from the trioxo ligand to the dinitrogen molecule to form the N_2O molecule coordinated to the O atom, is characterized by the lowest energy. However, the energy barrier (33.6 kcal mol^{-1}) remains high, although it is decreased by 9 kcal mol^{-1} compared to the negatively charged system. The same activation energy for **TS$_{13}$** is obtained when the trioxo group of complex **21** is used as an oxidizing species.

The next two groups of the adjacent transition states **TS$_7$**, **TS$_8$**, **TS$_9$** and **TS$_{10}$**, **TS$_{11}$**, **TS$_{12}$** are genetically related to the transition state **TS$_2$** and differ only by the type of its protonation. The states containing the hydroxo ligand (**TS$_9$**) or the hydroperoxo ligand involved in the direct oxygen atom transfer (**TS$_7$** and **TS$_8$**) are characterized by the lowest energy. The lowest activation barrier (20 kcal mol^{-1}) corresponds to the transition state **TS$_8$**, being 20.7 kcal mol^{-1} lower than the activation barrier for the transition state **TS$_2$** in the neutral system. Thus, the protonation of the vanadium peroxo complexes can considerably enhance their reactivity. The protonation of the peroxo group, which is not involved in the reaction, results in the higher-lying transition states corresponding to the higher activation barriers (~30 kcal mol^{-1}).

The activation barriers change slightly compared to that of the starting nonprotonated system for the transfer of the oxygen atom to the N_2 molecule from the open VO_5H form (**22**) through the intramolecular (**TS$_{14}$**) and intermolecular (**TS$_{15}$**) transition states. The only substantial difference is that **TS$_{15}$** is the fourth order saddle point, and all structures with one imaginary frequency are transformed into **TS$_{11}$** upon optimization. It should be noted that the energy of the transition state similar to **TS$_{15}$** for the negatively charged system with the linear O—O—N—N group, which is also characterized by four imaginary frequencies, is only 0.5 kcal mol^{-1} higher than the energy of **TS$_4$**.

Table 5. Total energies E and zero-point vibration energies ZPE of the vanadium complexes, transition states in the $VO_5H + N_2$ system calculated using the B3LYP method in the LANL2DZ basis set and in the extended E^* basis set, and relative energies Δ

Structure	$-E$	ZPE	$-E^*$	Δ /kcal mol^{-1}
	hartree			
16	47.99704	0.02520	48.09635	−13.1
17	47.97078	0.02658	48.08009	−2.1
18	47.96863	0.02438	48.07460	0
18T	47.96423	0.02334	48.06721	4.0
19	47.96182	0.02506	48.06786	4.7
20	47.95762	0.02599	48.06534	6.8
21	47.96393	0.02526	48.06102	9.1
22	47.92579	0.02444	48.02693	30.0
23	57.47689	0.03438	57.63845	−11.5
24	57.46927	0.03184	57.63000	−7.8
24T	57.45228	0.03074	57.61735	0.4
25	57.47129	0.03317	57.63007	−7.0
26	57.43691	0.03218	57.59062	17.2
TS$_6$	57.43926	0.03099	57.58402	20.5
TS$_7$	57.42937	0.03182	57.57710	25.4
TS$_8$	57.42600	0.03143	57.57454	26.8
TS$_9$	57.42724	0.03083	57.57301	27.4
TS$_{10}$	57.41862	0.03236	57.56313	34.5
TS$_{11}$	57.41616	0.03226	57.56099	35.8
TS$_{12}$	57.41255	0.03147	57.55526	38.9
TS$_{13}$	57.41042	0.03206	57.54976	42.7
TS$_{14}$	57.38973	0.03197	57.53674	50.8
TS$_{15}$	57.37670	0.02844	57.53113	58.6
27	57.47883	0.03409	57.64103	−13.3
28	57.47697	0.03356	57.63894	−12.3
29	72.84279	0.02197	72.92804	−2.8
30	57.45957	0.03506	57.62005	0.5
31	72.82039	0.02322	72.90453	12.7
32	72.80856	0.02256	72.89131	20.6

The oxidation of dinitrogen in the neutral $VO_5H + N_2$ system becomes more thermodynamically favorable, and the higher bond energy of the reaction product in the vanadium monoperoxo complex is observed. This correlates with the shortening of the V—O bond in complexes **28** and **30** (Fig. 12). However, in complex **27**, where N_2O is coordinated through the terminal N atom, on the contrary, the bond length is slightly (by 0.014 Å) elongated compared to that in complex **6**. A comparison of the energies of complexes **29**, **31**, and **32** shows the following: first, the protonation of the oxo group is more favorable in the case of the monoperoxo complexes than for the diperoxo complex and, second, the monodentate and bidentate coordinations of the hydroperoxo group differ slightly in the energy.

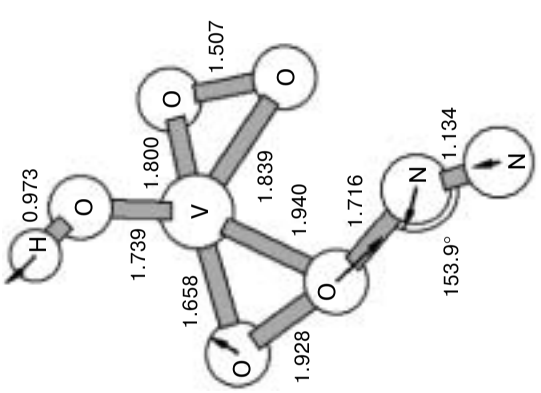

TS$_9$ 522i cm^{-1}

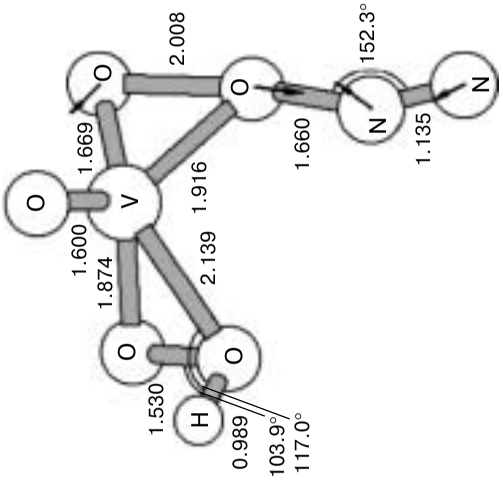

TS$_{10}$ 546i cm^{-1}

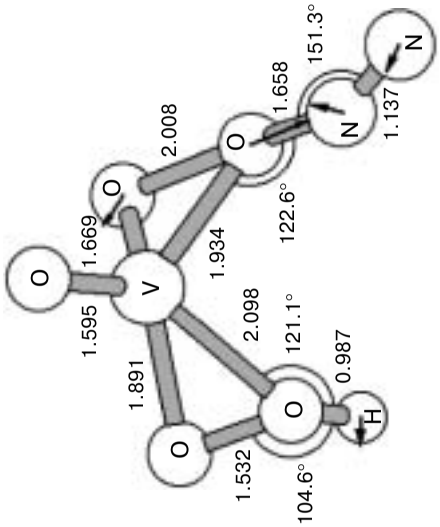

TS$_{11}$ 551i cm^{-1}

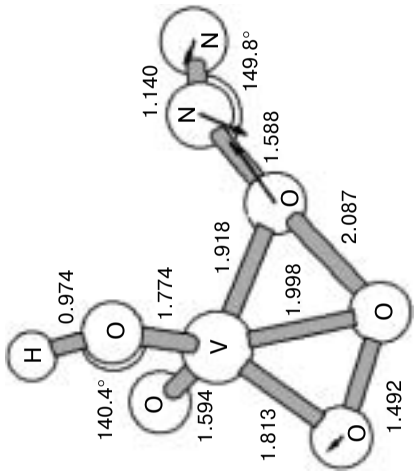

TS$_6$ 569i cm^{-1}

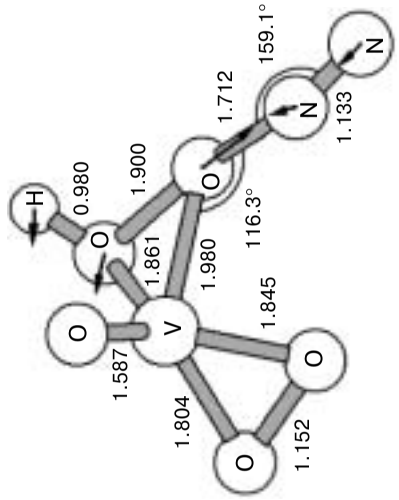

TS$_7$ 471i cm^{-1}

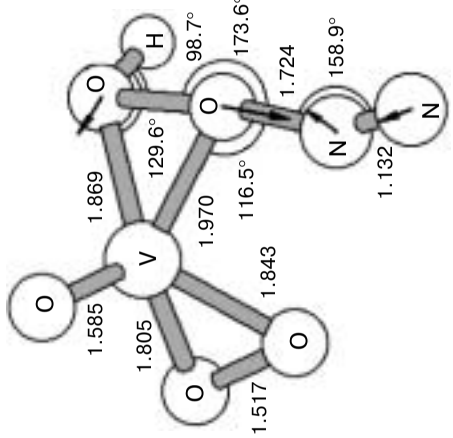

TS$_8$ 463i cm^{-1}

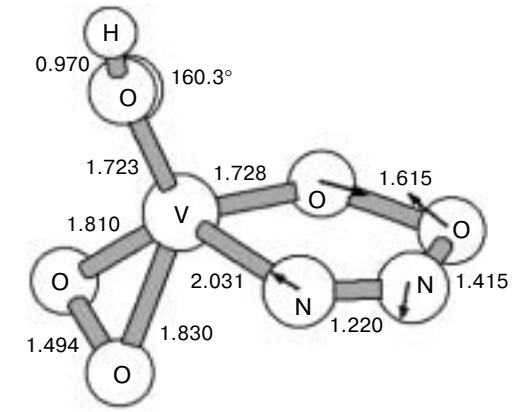

TS_{14} 430i cm^{-1}

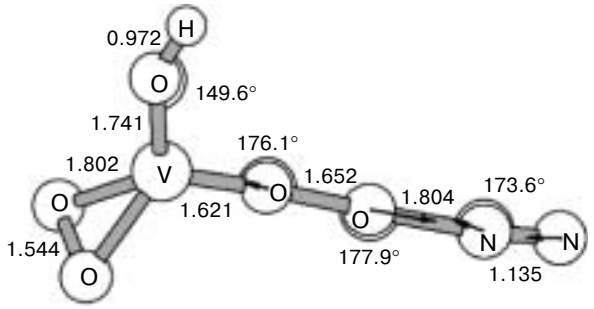

TS_{15} 649i cm^{-1}

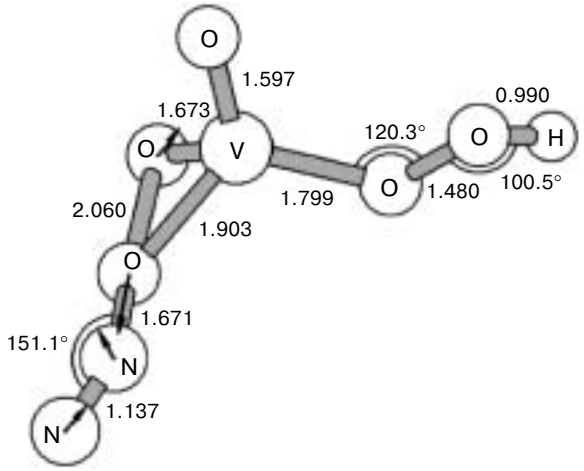

TS_{12} 526i cm^{-1}

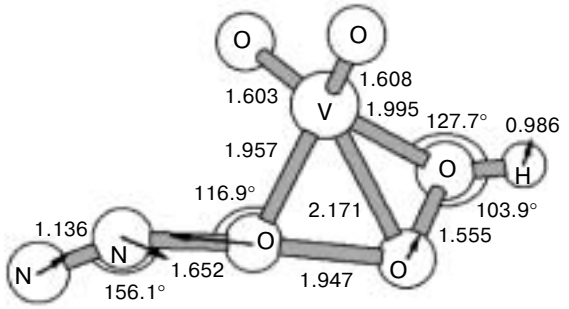

TS_{13} 503i cm^{-1}

Fig. 11. Structures of the transition states in the $VO_5H + N_2$ system. The arrows designate the displacements of the atoms for vibrations with the imaginary frequency.

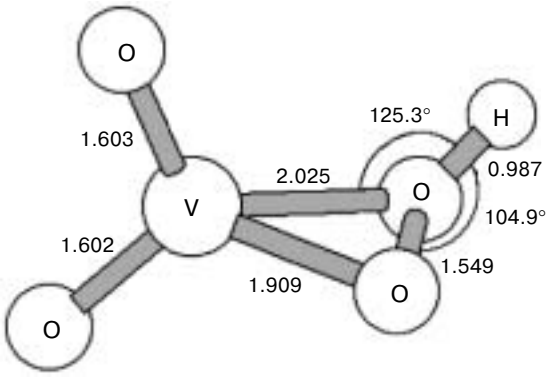

31

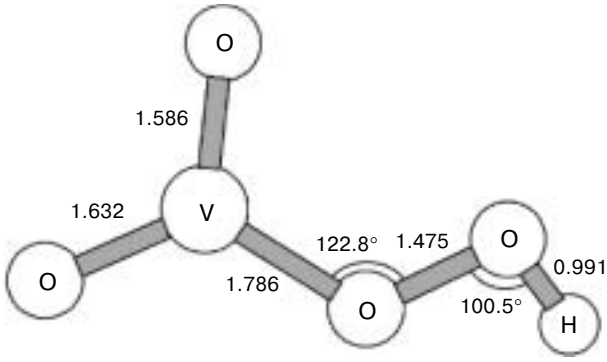

32

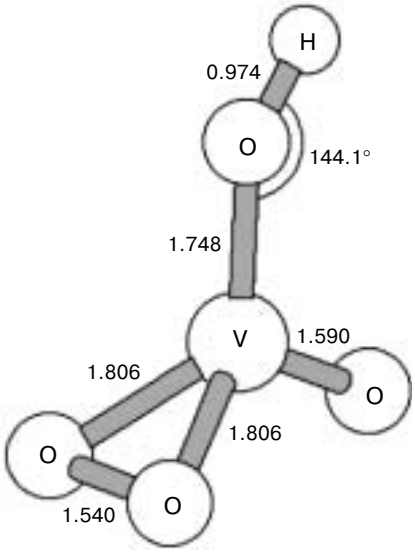

29

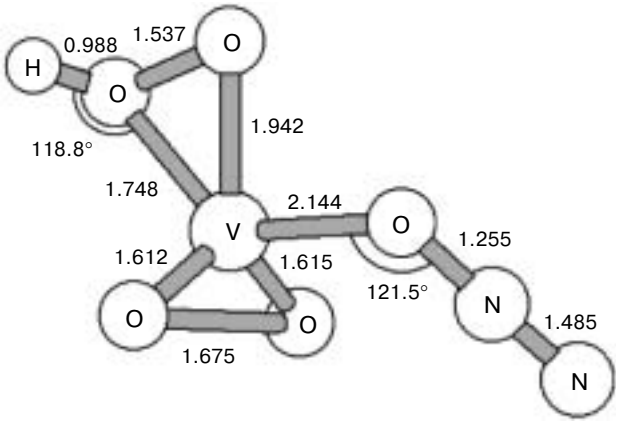

30

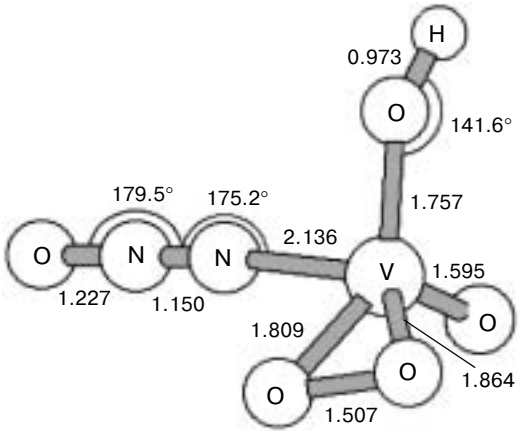

27

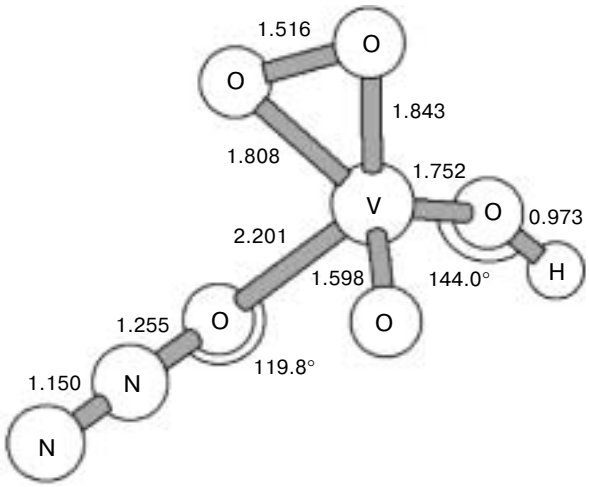

28

Fig. 12. Structure of the VO_4H and $VO_4H(N_2O)$ complexes.

Thus, the study of possible routes of dinitrogen oxidation with vanadium diperoxo complexes showed that the coordination of the solvent and the protonation of the complexes increase their reactivity toward the nitrogen molecule. This result explains qualitatively a possibility of easy N_2 oxidation in the $V^V—H_2O_2—CF_3COOH$ system. It would be of interest to study the combined effect of these factors. However, preliminary calculations showed that this is a very labor-consuming task because both the number of possible structures is greater and their localization is difficult for the formation of stable hydrogen bonds with several positions of equilibrium. In addition, a necessity to use the idealized gas-phase models for studying the reaction in solutions somewhat restricts their complication. Therefore, it seems most reasonable to perform experiments providing an information on the qualitative composition of the active species.

This work was financially supported by the Russian Foundation for Basic Research (Project No. 01-03-33076).

References

1. V. Conte, F. Di Furia, and G. Licini, *Appl. Catal. A: General*, 1997, **157**, 335.
2. A. Messerschmidt and R. Wever, *Proc. Natl. Acad. Sci. USA*, 1996, **93**, 392.
3. A. Messerschmidt, L. Prade, and R. Wever, *Biol. Chem.*, 1997, **378**, 309.
4. D. Rehder, *Coord. Chem. Rev.*, 1999, **182**, 297.
5. A. F. Shestakov and A. E. Shilov, *Izv. Akad. Nauk*, *Ser. Khim.*, 2001, 1963 [*Russ. Chem. Bull.*, *Int. Ed.*, 2001, **50**, 2054].
6. N. I. Moiseeva, A. E. Gekhman, and I. I. Moiseev, *Gazz. Chim. Ital.*, 1992, **122**, 187.
7. A. E. Gekhman, N. I. Moiseeva, and I. I. Moiseev, *Koord. Khim.*, 1992, **18**, 3 [*Russ. J. Coord. Chem.*, 1992, **18** (Engl. Transl.)].
8. A. E. Gekhman, N. I. Moiseeva, E. A. Blyumberg, and I. I. Moiseev, *Izv. Akad. Nauk SSSR, Ser. Khim.*, 1985, 2653 [*Bull. Acad. Sci. USSR, Div. Chem. Sci.*, 1985, **34**, 2458 (Engl. Transl.)].
9. A. E. Gekhman, N. I. Moiseeva, and I. I. Moiseev, *Izv. Akad. Nauk*, *Ser. Khim.*, 1995, 605 [*Russ. Chem. Bull.*, 1995, **44**, 584 (Engl. Transl.)].
10. A. E. Gekhman, I. P. Stolyarov, A. F. Shestakov, A. E. Shilov, and I. I. Moiseev, *Izv. Akad. Nauk*, *Ser. Khim.*, 2003, 733 [*Russ. Chem. Bull.*, *Int. Ed.*, 2003, **52**, 768].
11. M. J. Frisch, G. W. Trucks, M. Head-Gordon, P. M. W. Gill, M. W. Wong, J. B. Foresman, B. G. Johnson, H. B. Schlegel, M. A. Robb, E. S. Replogle, R. Gomperts, J. L. Andres, K. Raghavachari, J. S. Binkley, C. Gonzalez, R. L. Martin, D. J. Fox, D. J. Defrees, J. Baker, J. J. P. Stewart, and J. A. Pople, *GAUSSIAN-98*, *Revision A 6*, Gaussian, Inc., Pittsburgh (PA), 1998.
12. C. Djordjevic, N. Vuletic, M. L. Renslo, B. C. Puryear, and R. Alimard, *Mol. Cell. Biochem.*, 1995, **153**, 25.
13. V. Conte, O. Bortolini, M. Carraro, and S. Moro, *J. Inorg. Biochem.*, 2000, **80**, 41.
14. O. Bortolini, V. Conte, F. Di Furia, and S. Moro, *Eur. J. Inorg. Chem.*, 1998, **8**, 1193.
15. V. Conte, F. Di Furia, and S. Moro, *Inorg. Chim. Acta*, 1998, **272**, 62.
16. T. J. Won, C. L. Barnes, E. O. Schlemper, and R. C. Thompson, *Inorg. Chem*, 1995, **34**, 4499.
17. A. Butler, M. J. Clague, and G. E. Meister, *Chem. Rev.*, 1994, **94**, 625.
18. J. S. Jaswal and A. S. Tracey, *Inorg. Chem.*, 1991, **30**, 3718.
19. V. Sucha, M. Sivak, J. Tyrselova, and J. Marek, *Polyhedron*, 1997, **16**, 2837.
20. A. E. Lapshin, Y. E. Smolin, Y. F. Shepelev, D. Gyepesova, and P. Schwendt, *Acta Cryst. C*, 1989, **45**, 1477.
21. A. E. Lapshin, Y. E. Smolin, Y. F. Shepelev, P. Schwendt, and D. Gyepesova, *Acta Cryst. C*, 1990, **46**, 738.
22. P. Schwendt, A. Oravcova, J. Tyrselova, F. Pavelcik, and J. Marek, *Polyhedron*, 1996, **15**, 4507.
23. V. Conte, F. Di Furia, S. Moro, and S. Rabbolini, *J. Mol. Catal. A: Chem.*, 1996, **113**, 175.
24. V. Conte, F. DiFuria, and S. Moro, *J. Mol. Catal. A: Chem.*, 1997, **120**, 93.
25. A. Bagno, V. Conte, F. DiFuria, and S. Moro, *J. Phys. Chem. A*, 1997, **101**, 4637.
26. M. Bonchio, O. Bortolini, V. Conte, and S. Moro, *Eur. J. Inorg. Chem.*, 2001, 2913.
27. D. R. Drew and F. R. W. Einstein, *Inorg. Chem.*, 1972, **11**, 1079.
28. S. M. Vinogradova and A. F. Shestakov, *Koord. Khim.*, 1981, **7**, 974 [*Sov. J. Coord. Chem.*, 1981, **7** (Engl. Transl.)].
29. V. V. Strelets, *Elektrokhimiya*, 1992, **28**, 490 [*Russ. J. Electrochem.*, 1992, **28** (Engl. Transl.)].
30. F. Demartin, M. Biagioli, L. Strinna-Erre, A. Panzanelli, and G. Micera, *Inorg. Chim. Acta*, 2000, **299**, 123.
31. M. Casny and D. Rehder, *Chem. Commun.*, 2001, **10**, 921.

Received August 29, 2002;
in revised form March 24, 2003